Characterization of Two Dissimilatory Sulfite Reductases (Desulforubidin and Desulfoviridin) from the Sulfate-Reducing Bacteria. Mössbauer and EPR Studies

I. Moura,[†] J. LeGall,[‡] A. R. Lino,[†] H. D. Peck, Jr.,[‡] G. Fauque,[‡,⊥] A. V. Xavier,[†] D. V. DerVartanian,[‡] J. J. G. Moura,[†] and B. H. Huynh*[§]

Contribution from the Department of Physics, Emory University, Atlanta, Georgia 30322, Centro de Quimica Estrutural, Universidade Nova de Lisboa, Complexo I, IST, AV. Rovisco Pais, 1000 Lisboa, Portugal, and Department of Biochemistry, University of Georgia, Athens, Georgia 30602. *Received June 18, 1987*

Abstract: Mössbauer, EPR, optical, and biochemical techniques were used to characterize the prosthetic groups of two dissimilatory sulfite reductases: desulforubidin from *Desulfovibrio baculatus* strain DSM 1743 and desulfoviridin from *Desulfovibrio gigas*. For each molecule of desulforubidin, which has an $\alpha_2\beta_2$ configuration, there are two sirohemes and four [4Fe–4S] clusters. The [4Fe–4S] clusters are in the diamagnetic 2+ oxidation state and exhibit Mössbauer spectral properties similar to those of the oxidized *Bacillus stearothermophilus* ferredoxin. The sirohemes are high-spin ferric ($S = {}^5/_2$) and exhibit characteristic ferric heme EPR resonances at $g = 6.43$, 5.34, and 1.97. The Mössbauer parameters for the sirohemes ($\Delta E_Q = 1.94 \pm 0.03$ mm/s and $\delta = 0.42 \pm 0.02$ mm/s at 195 K) are consistent with a high-spin ferric heme assignment. The Mössbauer measurements further demonstrate that each siroheme is exchange-coupled to a $[4Fe–4S]^{2+}$ cluster. Such an exchange-coupled siroheme–[4Fe–4S] unit has also been found in the assimilatory sulfite reductase from *Escherichia coli* (Christner, J. A., et al. *J. Biol. Chem.* **1981**, *256*, 2098–2101) and in a low molecular weight sulfite reductase from *Desulfovibrio vulgaris* (Huynh, B. H., et al. *J. Biol. Chem.* **1984**, *259*, 15373–15376). Detailed data analysis suggests that even though the siroheme and the exchange-coupled [4Fe–4S] cluster in desulforubidin have spectral properties distinctively different from those of *E. coli* sulfite reductase, the exchange-coupling mechanism appears to be the same in both enzymes. Desulforubidin can be reduced under a hydrogen atmosphere in the presence of trace amounts of hydrogenase and methylviologen. The reducing electron was found to reside on the siroheme. The Mössbauer parameters for the reduced siroheme ($\Delta E_Q = 2.72 \pm 0.05$ mm/s and $\delta = 0.92 \pm 0.03$ mm/s at 4.2 K) indicate that it is in a high-spin ferrous ($S = 2$) state. The electronic states of the exchange-coupled and the uncoupled [4Fe–4S] clusters are unaltered under this reducing condition. The most exciting and curious results were obtained from the studies of desulfoviridin. We found that for each molecule of desulfoviridin there are two tetrahydroporphyrin groups and four $[4Fe–4S]^{2+}$ clusters. Most surprisingly, about 80% of the tetrahydroporphyrin groups do not contain iron. With the assumption that each molecule can have up to two tetrapyrrolic groups, our finding suggests that 60–80% of the purified desulfoviridin molecules may contain only metal-free tetrahydroporphyrins while 40–20% of the molecules may contain one to two sirohemes. Interestingly, the sirohemes are also exchange-coupled to $[4Fe–4S]^{2+}$ clusters. Implications for the existence of metal-free tetrahydroporphyrins in the purified enzymes are discussed. Spectroscopic properties for the iron-containing prosthetic groups in desulfoviridin are essentially the same as those reported for desulforubidin. In addition to the tetrapyrrolic groups and the [4Fe–4S] clusters, a solitary iron center was also found in both dissimilatory sulfite reductases. In the as-purified reductases, this solitary iron is high-spin ferric. In the reduced enzymes, it is high-spin ferrous. The Mössbauer parameters for the reduced iron ($\Delta E_Q = 3.2$ mm/s and $\delta = 1.25$ mm/s at 4.2 K) are consistent with octahedrally coordinated Fe(II) compounds with oxygenous and/or nitrogenous ligands. Whether this iron is adventitiously bound to the protein or has any physiological role is presently unclear.

A variety of sulfite reductases have been purified from the sulfate-reducing bacteria: (1) desulfoviridins from *Desulfovibrio* (*D.*) *gigas*, *D. salexigens*, and *D. vulgaris*,[1-3] (2) desulforubidins from *D. baculatus* strains Norway 4 and DSM 1743,[4] (3) P-582 from *Desulfotomaculum* (*Dt.*) *ruminis* and *Dt. nigrificans*,[5,6] and (4) desulfofuscidins from *D. thermophilus*[7] and *Thermodesulfobacterium commune*.[8] These sulfite reductases are involved in the pathway of respiratory sulfate reduction and are termed "dissimilatory" sulfite reductases. Another class of sulfite reductase is called "assimilatory" sulfite reductase whose function is to provide reduced sulfur for the synthesis of sulfur-containing cell constituents. A third class of sulfite reductase is found in several strictly anaerobic bacteria and has been termed "assimilatory-type" sulfite reductase.[2] This class of enzymes is characterized by the presence of a ferric low-spin siroheme exchange-coupled to a [4Fe–4S] cluster in a relatively small (~25 kDa) polypeptide chain.[9,10] In the presence of reduced methylviologen, both the assimilatory sulfite reductase and the assimilatory-type sulfite reductase can catalyze the six-electron reduction of sulfite to sulfide without the formation of free intermediates. On the other hand, the dissimilatory sulfite reductase reduces sulfite to sulfide with accumulation of trithionate and thiosulfate; however, the production of these intermediates is an irreversible process and may not occur in intact cells.

The physical properties of the various dissimilatory sulfite reductases are quite similar in general, but different in details. They are large oligomers with molecular mass in the order of 200 kDa and are composed of two different types of subunits organized in an $\alpha_2\beta_2$ configuration. Each enzyme was reported to contain approximately 14–16 non-heme iron atoms and comparable

[†] Universidade Nova de Lisboa.
[‡] University of Georgia.
[§] Emory University.
[⊥] Present address: ARBS, C.E.N. Cadarache, 13108 St. Paul-Lez-Durance, Cedex, France.

(1) Lee, J. P.; Peck, H. D., Jr. *Biochem. Biophys. Res. Commun.* **1971**, *45*, 583–586.
(2) Lee, J. P.; LeGall, J.; Peck, H. D., Jr. *J. Bacteriol.* **1973**, *115*, 529–542.
(3) Czechowski, M.; Fauque, G.; Galliano, N.; Dimon, B.; Moura, I.; Moura, J. J. G.; Xavier, A. V.; Barata, B. A. S.; Lino, A. R.; LeGall, J. *J. Ind. Microbiol.* **1986**, *1*, 139–147.
(4) Lee, J. P.; Yi, C.; LeGall, J.; Peck, H. D., Jr. *J. Bacteriol.* **1973**, *115*, 453–455.
(5) Trudinger, P. A. *J. Bacteriol.* **1970**, *104*, 158–170.
(6) Akagi, J. M.; Adams, V. *J. Bacteriol.* **1973**, *116*, 392–396.
(7) LeGall, J.; Fauque, G. *Biology of Anaerobic Microorganisms*; Zehnder, A. J. B., Ed.; Wiley: New York, in press.
(8) Hatchikian, E. C.; Zeikus, J. G. *J. Bacteriol.* **1983**, *153*, 1211–1220.
(9) Huynh, B. H.; Kang, L.; DerVartanian, D. V.; Peck, H. D., Jr.; LeGall, J. *J. Biol. Chem.* **1984**, *259*, 15373–15376.
(10) Moura, I.; Lino, A. R.; Moura, J. J. G.; Xavier, A. V.; Fauque, G.; Peck, H. D., Jr.; LeGall, J. *Biochem. Biophys. Res. Commun.* **1986**, *141*, 1032–1041.

0002-7863/88/1510-1075$01.50/0

amounts of labile sulfide.[11] Their optical spectra show typical siroheme bands in the region 540–580 nm and around 400 nm. An additional absorption maximum at 628 nm was observed for desulfoviridin.[8,12,13] Curiously, the non-heme iron does not contribute significantly to the optical spectrum and is difficult to reduce. The EPR spectra of these reductases show characteristic high-spin ferric-heme-type EPR signals in the $g \sim 6$ and 2 regions; however, significant differences in their g values were observed.[11,14] Upon treatment of acetone/HCl, heme chromophore can be extracted from desulforubidin, desulfofuscidin, and P-582 with spectral properties identical with those of the extracted siroheme from *Escherichia (E). coli* sulfite reductase,[8,12,15] and approximately two sirohemes were found for each enzyme molecule. However, under the same conditions the chromophore extracted from desulfoviridin showed spectral properties of sirohydrochlorin (tetrahydroprophyrin; demetalized siroheme).[12,13] Approximately two sirohydrochlorins were extracted from each reductase.

The mechanism of sulfite reductase is not yet perfectly understood; in particular, the functional roles of the sirohemes and the iron–sulfur clusters have not yet been determined. The latter may not be essential for the reduction of sulfite, since it has been demonstrated that isolated sirohydrochlorin plus iron, or siroheme, is capable of reducing sulfite.[16,17] In the case of siroheme, the reduced product is exclusively trithionate. The amount of sulfite reduced is proportional to the amount of siroheme present in the reaction mixture, and each molecule of siroheme performs only 300 catalytic cycles.[18] These observations point to a possible regulatory role of the iron–sulfur clusters to ensure proper internal electron transfer in the enzyme molecule.

In this paper we report a detailed Mössbauer investigation of two different sulfite reductases, namely, desulforubidin from *D. baculatus* and desulfoviridin from *D. gigas*. In order to better characterize the prosthetic groups, we have also studied the EPR spectra and determined the iron and heme contents of the ^{57}Fe-enriched enzymes. We found that desulforubidin contains exchange-coupled siroheme–[4Fe–4S] units which are similar to those found in the hemoprotein subunit of *E. coli* sulfite reductase.[19] To our surprise, we discovered that the majority of the purified desulfoviridin contains demetalized sirohydrochlorin, with only a minor portion of the sample containing siroheme. The siroheme in desulfoviridin was also found to be coupled with a [4Fe–4S] cluster.

Methods

Growth of Organisms and Preparation of Crude Extracts. ^{57}Fe-enriched cells of *D. gigas* NCIB 9332 and *D. baculatus* DSM 1743 were grown in lactate–sulfate media as previously described.[20] The medium contained 0.5 mg of ^{57}Fe (95% enrichment, New England Nuclear) per L. Cells from 400 L were harvested by centrifugation at the end of the exponential growth phase and stored at −80 °C. Approximately 300 g wet weight of *D. gigas* or *D. baculatus* cells was suspended in 300 mL of 10 mM pH 7.6 Tris-HCl buffer, DNase was added, and the cells were ruptured in a French press at 62 MPa. The extract was then centrifuged at 12000 rpm for 30 min, and a total volume of 500 mL of crude cell extract was obtained.

Purification of Desulfoviridin from *D. gigas*. All purification procedures were carried out in air at 5 °C, and the pH of the buffers was 7.6 (measured at 20 °C for Tris-HCl).

The crude cell extract was adsorbed on a DEAE-cellulose (DE52) column (5 × 36 cm), and the proteins were eluted with a continuous gradient of 10–500 mM Tris-HCl buffer (2 L). A green solution containing the desulfoviridin fraction was recovered between 250 and 300 mM Tris-HCl. This green fraction was dialyzed overnight against 20 L of distilled water and adsorbed on a DEAE-Biogel A column (4 × 25 cm). After elution with a continuous gradient of 10–300 mM Tris-HCl buffer (1.5 L), a protein solution containing desulfoviridin was collected in a volume of 600 mL. This protein solution yielded an absorption ratio of $A_{280}/A_{628} = 7.5$. After dialysis the proteins were again placed on a second DEAE-Biogel A column identical with the previous one. The same gradient was performed, and the protein solution collected at this stage had an A_{280}/A_{628} ratio of 4.8. A final step of purification was performed on a hydroxylapatite column (2.5 × 20 cm) equilibrated with 300 mM Tris-HCl. A linear Tris-HCl gradient from 300 to 10 mM (0.5 L) was applied to the column, and the protein desulfoviridin was eluted with a continuous potassium phosphate gradient of 1–100 mM (1 L). The purified desulfoviridin had an A_{280}/A_{628} ratio of 4.0.

Purification of Desulforubidin from *D. baculatus*. The crude cell extract was adsorbed on a DEAE-Biogel A column (5 × 50 cm), and a continuous gradient of Tris-HCl buffer from 10 to 400 mM (2 L) was applied. A red protein solution of 500 mL containing desulforubidin was collected between 250 and 300 mM Tris-HCl. This red fraction was dialyzed against distilled water overnight and was adsorbed on a second DEAE-Biogel A column (5 × 50 cm). The same gradient of Tris-HCl was applied, and a desulforubidin fraction collected at this stage had an A_{280}/A_{543} of 9.6. The fraction was concentrated in an Amicon Diaflo ultrafilter with a YM 30 membrane. The concentrated solution was passed on a Spherogel TSK-G-3000 preparative column in an HPLC apparatus, and the protein was eluted with a 0.1 M phosphate buffer, pH 7.0, containing 0.1 M NaCl. The purified desulforubidin had an A_{280}/A_{543} ratio of 7.1.

Protein Determination. The protein concentration was determined by the method of Lowry et al.[21] with the Folin–ciocalteu phenol reagent. Bovine serum albumin was used as standard.

Iron Determination. The total iron content was determined by plasma emission spectroscopy using a Jarrel-Ash Model 750 and by forming a ferrous complex with 2,4,6-tripyridyl-*s*-triazine using the method described by Fisher and Price.[22]

Determination of Siroheme or Sirohydrochlorin Content. The classical method of Siegel et al.[23] was used to extract siroheme or sirohydrochlorin from the sulfite reductases. To each volume of enzyme solution, nine volumes of ice-cold acetone/HCl (15 mM in acetone) were added. After vigorous mixing, the mixture was allowed to stand for 5 min at 0 °C and was then centrifuged at high speed to remove the protein precipitate. To stabilize the extracted chromophore, 0.5 volume of pyridine was added to each volume of the extracted solution. The pyridine chromophore solution was centrifuged and its absorption spectrum measured.

Optical, EPR, and Mössbauer Methods. Optical absorption spectra were recorded on a Shimadzu Model 260 spectrophotometer. EPR spectra were recorded on a Bruker ER-200 tt spectrometer equipped with an Oxford Instruments continuous-flow cryostat. Both the low- and high-field Mössbauer spectrometers are of the constant-acceleration types and have been described previously.[24] The zero velocity was referred to the centroid of the room-temperature Mössbauer spectrum of a metallic iron foil.

Results

Iron Content. Four preparations of each dissimilatory sulfite reductase were used for iron determinations. Applying plasma-emission spectroscopy and chemical methods, the total iron contents were found to be 21 ± 2 mol of iron per mol of desulforubidin and 18 ± 2 mol of iron per mol of desulfoviridin. The lower value for desulfoviridin is consistent with the following EPR and Mössbauer data, which show that a majority of the desulfoviridin molecules contain metal-free sirohydrochlorin. The EPR and Mössbauer data also indicate that the purified desulfoviridin and desulforubidin contain approximately 5–6% solitary non-heme high-spin ferric iron.

Siroheme and Sirohydrochlorin Determinations. Four preparations of each sulfite reductase were used for chromophore ex-

(11) Liu, C. L.; DerVartanian, D. V.; Peck, H. D., Jr. *Biochem. Biophys. Res. Commun.* **1979**, *91*, 962–970.
(12) Murphy, M. J.; Siegel, L. M. *J. Biol. Chem.* **1973**, *248*, 6911–6919.
(13) Murphy, M. J.; Siegel, L. M.; Kamin, H.; DerVartanian, D. V.; Lee, J. P.; LeGall, J.; Peck, H. D., Jr. *Biochem. Biophys. Res. Commun.* **1973**, *54*, 82–88.
(14) Hall, M. H.; Prince, R. H.; Cammack, R. *Biochim. Biophys. Acta* **1979**, *581*, 27–33.
(15) Murphy, M. J.; Siegel, L. M.; Kamin, H.; Rosenthal, D. *J. Biol. Chem.* **1973**, *248*, 2801–2814.
(16) Seki, Y.; Sogawa, N.; Ishimoto, M. *J. Biochem. (Tokyo)* **1981**, *90*, 1487–1492.
(17) Seki, Y.; Ishimoto, M. *J. Biochem. (Tokyo)* **1979**, *86*, 273–276.
(18) Kang, L.; LeGall, J.; Kowal, A. T.; Johnson, M. K. *J. Inorg. Chem.*, in press.
(19) Christner, J. A.; Münck, E.; Janick, P. A.; Siegel, L. M. *J. Biol. Chem.* **1981**, *256*, 2098–2101.
(20) Huynh, B. H.; Czechowski, M. H.; Krüger, H. J.; DerVartanian, D. V.; Peck, H. D., Jr.; LeGall, J. *Proc. Natl. Acad. Sci. U.S.A.* **1984**, *81*, 3728–3732.
(21) Lowry, O. H.; Rosebrough, N. J.; Fan, A. L.; Randall, R. J. *J. Biol. Chem.* **1951**, *193*, 265–275.
(22) Fisher, D. S.; Price, D. C. *Clin. Chem.* **1964**, *10*, 21–25.
(23) Siegel, L. M.; Murphy, M. J.; Kamin, H. *Methods Enzymol.* **1978**, *52*, 436–447.
(24) Yang, C. Y.; Meagher, A.; Huynh, B. H.; Sayers, D. E.; Thiel, E. C. *Biochemistry* **1987**, *26*, 497–503.

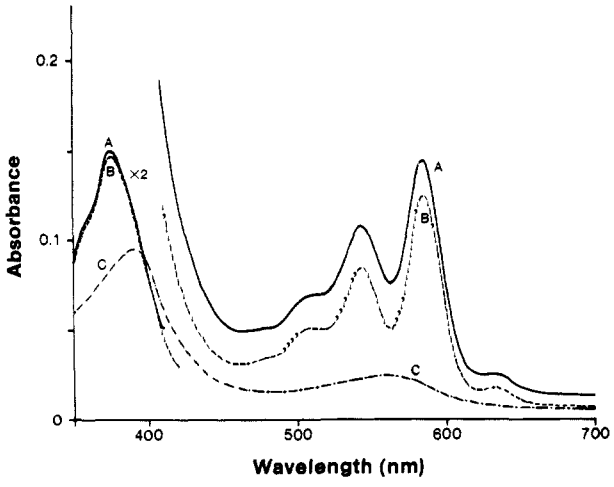

Figure 1. Absorption spectra of the tetrapyrrolic chromophores extracted from *D. gigas* desulfoviridin (trace A) and from *D. baculatus* desulforubidin (trace C). Spectrum C is normalized to 25% of the chromophore concentration of the sample in A. Trace B is the difference spectrum of spectra A and C.

tractions (see Methods). The extracted chromophores were allowed to complex with pyridines, and their concentrations were determined by optical spectroscopy. The extinction coefficients $\epsilon_{557} = 1.57 \times 10^4$ M^{-1} cm^{-1} and $\epsilon_{588} = 2.4 \times 10^4$ M^{-1} cm^{-1} were used for siroheme and porphyrin methyl ester in pyridine, respectively.[13] A total of 2.2 ± 0.3 mol of siroheme was extracted per mol of desulforubidin, and 2.0 ± 0.2 mol of sirohydrochlorin was found for each mol of desulfoviridin. The following Mössbauer and EPR data indicate that 75–80% of the tetrapyrrolic chromophores in the purified desulfoviridin contain metal-free sirohydrochlorin while 20–25% contain iron atoms. To examine whether this finding is compatible with the optical data, the spectra of the extracted chromophores were studied in more detail. Figure 1 shows the optical spectrum of the extracted desulfoviridin chromophore (trace A). Characteristic absorption maxima for sirohydrochlorin at 378, 510, 545, 588, and 638 nm are observed. Trace C is a spectrum of the extracted desulforubidin chromophore (siroheme) normalized to 25% of the sirohydrochlorin concentration of the sample which yielded spectrum A. This 25% siroheme contribution is then subtracted from spectrum A, and the resulting spectrum is shown as trace B. When traces A and B are compared, it becomes obvious that the extracted desulfoviridin chromophore could have contained a minor amount of siroheme, and it would be difficult to detect by optical spectroscopy.

EPR. In the earlier preparations, multiple EPR-active species were reported for dissimilatory sulfite reductases.[11,14] The recently purified ^{57}Fe-enriched enzymes yielded much cleaner EPR spectra, even though multiple species remain visible. In Figure 2, a low-temperature EPR spectrum of the purified desulforubidin from *D. baculatus* is compared with a spectrum of *D. gigas* desulfoviridin. High-spin ferric-heme-type EPR signals are observed for both enzymes. For desulforubidin (spectrum 2A) resonances of the major component are detected at $g = 6.43$, 5.34, and 1.97, and a minor component is detected at $g = 6.94$, ~5.0, and ~1.9. The minor component is quantitated to be less than 10% of the major component. For desulfoviridin (spectrum 2B), two EPR-active species are observed. The major resonances at $g = 7.20$, 4.95, and 1.93 are attributed to the siroheme. The small signal at $g = 5.8$ is most probably originating from the excited state of the siroheme, since its intensity relative to the $g = 7.20$ signal declines with decreasing temperature. The identity of the species with resonance at $g = 9.7$ is presently unclear. The large g value indicates that it is not originating from a heme species and is consistent with a rhombic ($E/D = 0.33$) $S = {}^5/_2$ system. From the following Mössbauer data, we believe that the signal at $g = 9.7$ may represent a high-spin Fe(III) species. This same Fe(III) signal with comparable intensity is also detected for desulforubidin (see Figure 2A). In comparison with the EPR spectrum of *E. coli* sulfite reductase,[25] the heme spectra show different rhombicities, indicating structural differences for the sirohemes in these enzymes.

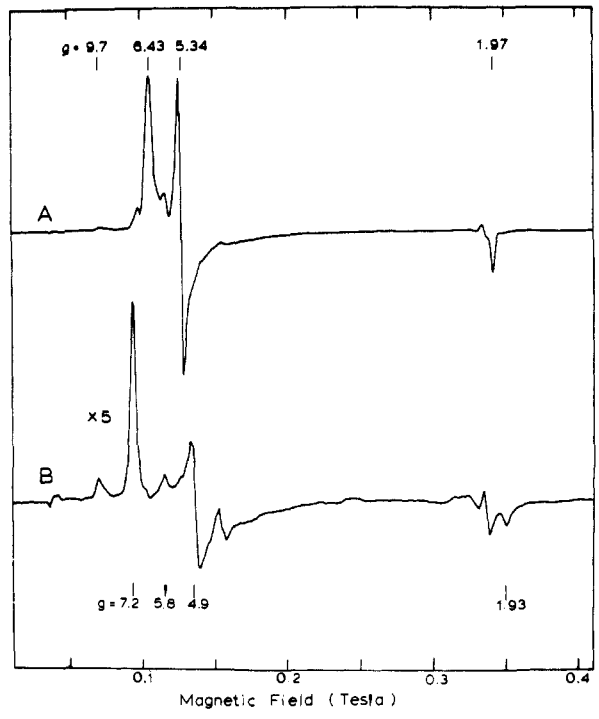

Figure 2. EPR spectra of dissimilatory sulfite reductases isolated from *D. baculatus* (desulforubidin, trace A) and *D. gigas* (desulfoviridin, trace B). Experimental conditions: microwave power, 2 mW; modulation amplitude, 1 mT; temperature, 8 K; microwave frequency, 9.43 GHz; receiver gain, 2×10^4 for A and 1×10^5 for B.

Since spectrum 2B was recorded with a gain of 5 times larger than that in spectrum 2A, it followed then that the EPR intensity of desulfoviridin should be approximately 5 times weaker than that of desulforubidin. After normalizing the EPR intensities with respect to protein concentrations and correcting for the Aasa and Vänngård factor,[26] we found that the concentration of EPR-active siroheme in desulfoviridin was only 25% of that in desulforubidin. This finding is in good agreement with the Mössbauer data presented below.

Low-Temperature Mössbauer Studies of Native Proteins. Figure 3A shows a Mössbauer spectrum of the as-purified desulforubidin from *D. baculatus*. The spectrum was recorded at 4.2 K with a magnetic field of 50 mT applied parallel to the γ-rays. The magnetic subspectral component extending from −4 to +4 mm/s arises from the high-spin ferric siroheme, and the peaks at −1.1 and +2.0 mm/s are indicative of an $[4Fe-4S]^{2+}$ cluster exchange-coupled to the paramagnetic siroheme. (Detailed analysis of the spectra of the exchange-coupled siroheme–[4Fe–4S] unit will be given in a following section.) Similar spectra have been reported for the siroheme–[4Fe–4S] unit in the hemoprotein subunit of *E. coli* sulfite reductase.[19] The broad central doublet has parameters (apparent quadrupole splitting $\Delta E_Q = 1.1$ mm/s and isomer shift $\delta = 0.43$ mm/s) characteristic of an $[4Fe-4S]^{2+}$ cluster. Spectra recorded at strong applied fields (see Figure 4A) indicate that this [4Fe–4S] cluster is diamagnetic and therefore not coupled to the siroheme. The relative absorption intensities for the coupled [4Fe–4S] cluster and the uncoupled [4Fe–4S] cluster are about 1:1. From the EPR studies, we realize that there exists also a rhombic high-spin Fe(III) species. The existence of this Fe(III) species can be detected in spectra recorded at strong applied fields (e.g., see Figure 4), but is not obvious in weak-field spectra (e.g., Figure 3A). With so many species present, a precise quantitation obviously cannot be achieved from spectrum 3A alone.

(25) Rueger, D. C.; Siegel, L. M. In *Flavins and Flavoproteins*; Singer, T. P., Ed.; Elsevier: Amsterdam, 1976; pp 610–620.
(26) Aasa, R.; Vänngård, T. *J. Magn. Reson.* **1975**, *19*, 308–315.

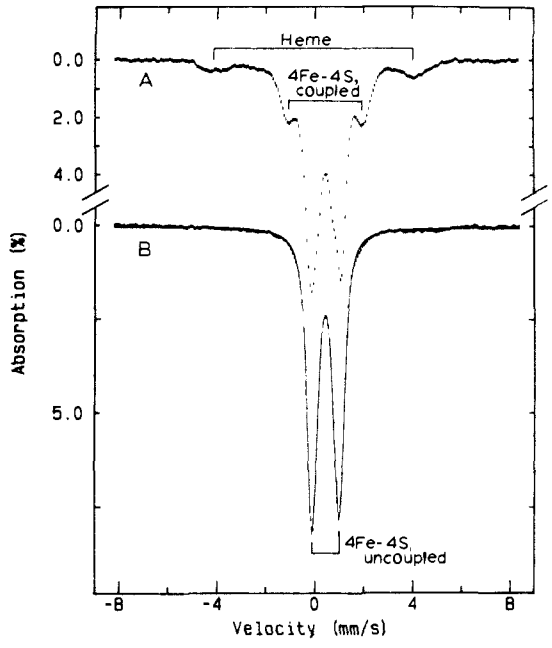

Figure 3. Mössbauer spectra of the as-isolated desulforubidin from *D. baculatus* (A) and desulfoviridin from *D. gigas* (B). The data were recorded at 4.2 K in a magnetic field of 50 mT applied parallel to the γ-beam. The three resolved spectral subcomponents are indicated by the brackets. The spectrum of the rhombic Fe(III) species is not resolved. The solid line in B is the results of a least-squares fit of four quadrupole doublets with equal intensity. Parameters resulting from the fit are listed in Table I.

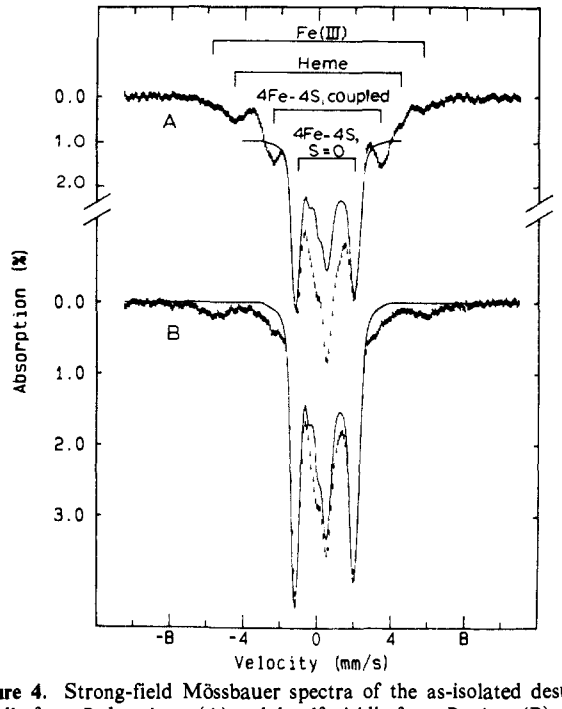

Figure 4. Strong-field Mössbauer spectra of the as-isolated desulforubidin from *D. baculatus* (A) and desulfoviridin from *D. gigas* (B). The data were recorded at 4.2 K in a parallel applied field of 8 T. The spectral components of the four different iron centers are resolved under these experimental conditions and are marked by the brackets. The solid lines are theoretical simulations of the diamagnetic, uncoupled [4Fe–4S]$^{2+}$ clusters. Parameters obtained from the least-squares fit of the weak-field spectrum (Figure 3B) were used in the simulations. The theoretical spectrum in A is normalized to 42% of the total iron absorption and it is normalized to 80% in B.

However, by analyzing data of the native enzyme recorded at different temperatures and applied fields and by correlating with data of the reduced enzyme (see below), we were able to obtain quantitative results. We found that the relative Mössbauer absorption for the siroheme is 10 ± 2%, for the coupled [4Fe–4S] cluster 42 ± 3%, for the uncoupled [4Fe–4S] cluster 42 ± 3%, and for the rhombic Fe(III) species 6 ± 1%. Combining these quantitative data with the results of iron content determination, we concluded that each molecule of desulforubidin contains two exchange-coupled siroheme–[4Fe–4S] units, two uncoupled [4Fe–4S]$^{2+}$ clusters, and approximately one rhombic high-spin Fe(III) species.

Figure 3B shows a Mössbauer spectrum of desulfoviridin from *D. gigas* recorded under the same experimental conditions as in spectrum 3A. The majority of the absorptions appear to be originating from the uncoupled [4Fe–4S]$^{2+}$ cluster. Most surprisingly, the spectrum corresponding to a siroheme–[4Fe–4S] unit is not observable, indicating that either the coupled unit has a fast electronic relaxation rate and therefore exhibits quadrupole doublets or the presence of such a unit in desulfoviridin is minor! In order to exclude the possibility of fast relaxation, we recorded spectra at strong applied fields. (Regardless of electronic relaxation rate, the internal field of a paramagnetic species will reach its saturation value when a strong magnetic field is applied, resulting in a magnetic spectrum that is easily distinguishable from a diamagnetic system.) Figure 4 shows the Mössbauer spectra of desulforubidin (4A) and desulfoviridin (4B) recorded at 4.2 K in a parallel applied field of 8 T. A close examination of the spectrum of desulforubidin reveals that the subspectral components corresponding to the four different iron species in the enzyme are partially resolved: The siroheme has absorption peaks at velocities −4.4 and +4.5 mm/s, the coupled [4Fe–4S] cluster at −2.3 and +3.4 mm/s, the uncoupled [4Fe–4S] cluster at −1, +0.5, and +2 mm/s, and the rhombic high-spin Fe(III) species at −5.6 and +5.8 mm/s. In comparison of spectrum 4B with spectrum 4A and with the simulated diamagnetic spectrum (see below), it becomes evident that the majority of the Mössbauer absorption of desulfoviridin can be attributed to diamagnetic uncoupled [4Fe–4S] clusters, and the siroheme content is very minor. Since the spectrum of the siroheme is magnetically split in the native enzyme, it is not surprising that we could not detect the presence of a small quantity of siroheme in spectrum 3B or 4B. Nevertheless, the existence of siroheme in desulfoviridin is evident from the EPR measurements and from the Mössbauer measurements of the reduced enzyme reported in the following section. An accurate quantitation of the siroheme absorption is derived from the spectra of the reduced enzyme, which indicates 2% absorption. Most interestingly, in spectrum 4B there are shoulders appearing at around −2.3 and +3.4 mm/s. Since only the coupled [4Fe–4S] cluster exhibits absorptions at these velocity regions, the observation of these shoulders indicates that the sirohemes in desulfoviridin, regardless of the small quantity, are also exchange-coupled to [4Fe–4S] clusters. Similar to desulforubidin, desulfoviridin also contains the rhombic high-spin Fe(III) species, which exhibits absorptions at −5.6 and +5.8 mm/s. An approximately equal amount of this Fe(III) species (5–6% of total iron absorption) is observed for both sulfite reductases.

From the above discussions, we realize that over 90% of the Mössbauer absorptions of native desulfoviridin arise from [4Fe–4S]$^{2+}$ clusters. In order to better characterize the [4Fe–4S]$^{2+}$ cluster, we analyzed the desulfoviridin spectra in detail. We first performed a least-squares fit to the 4.2 K weak-field spectrum of native desulfoviridin (Figure 3B). For simplicity it was assumed that the contributions from the minor species do not affect the spectrum significantly, and the data were fitted with four quadrupole doublets of equal intensity and line width. The parameters obtained (listed in Table I) are very similar to those reported for [4Fe–4S]$^{2+}$ clusters in reduced HiPIP[27] and oxidized ferredoxin.[28] In order to prove that the majority of the [4Fe–4S] clusters in desulfoviridin are diamagnetic, we used the results obtained from the least-squares fit and simulated the corresponding strong-field spectra assuming diamagnetism for the iron sites. The solid line

(27) Middleton, P.; Dickson, D. P. E.; Johnson, C. E.; Rush, J. D. *Eur. J. Biochem.* **1980**, *104*, 289–296.
(28) Middleton, P.; Dickson, D. P. E.; Johnson, C. E.; Rush, J. D. *Eur. J. Biochem.* **1978**, *88*, 135–141.

Table I. Mössbauer Parameters for the $[4Fe-4S]^{2+}$ Clusters in the As-Purified *D. baculatus* Desulforubidin and *D. gigas* Desulfoviridin

	desulfoviridin		desulforubidin	
	ΔE_Q, mm/s	δ, mm/s	ΔE_Q, mm/s	δ, mm/s
		T = 195 K		
siroheme			1.94 ± 0.03	0.42 ± 0.02
[4Fe-4S]				
site 1	1.13 ± 0.04	0.36 ± 0.02	1.10 ± 0.04	0.36 ± 0.02
site 2	0.91 ± 0.04	0.35 ± 0.02	0.98 ± 0.04	0.37 ± 0.02
site 3	0.80 ± 0.04	0.37 ± 0.02	0.83 ± 0.04	0.37 ± 0.02
site 4	0.50 ± 0.04	0.35 ± 0.02	0.51 ± 0.04	0.36 ± 0.02
		T = 4.2 K		
[4Fe-4S]				
site 1	1.45 ± 0.04	0.45 ± 0.02		
site 2	1.10 ± 0.04	0.45 ± 0.02		
site 3	1.10 ± 0.04	0.45 ± 0.02		
site 4	0.72 ± 0.04	0.41 ± 0.02		

in Figure 4B is the result of such a simulation. The good agreement between theory and experiment indicates that the majority of the $[4Fe-4S]^{2+}$ clusters in desulfoviridin are indeed diamagnetic.

The same theoretical spectrum is also plotted in Figure 4A to compare with the spectrum of the uncoupled [4Fe–4S] clusters in desulforubidin. The theoretical spectrum is normalized to 42% of the total Mössbauer absorption. From such a comparison, it becomes obvious that the spectrum of the uncoupled [4Fe–4S] cluster in desulforubidin may be approximated by the theoretical simulation using parameters obtained from the desulfoviridin analysis. This finding enables us to prepare spectra representing the coupled siroheme–[4Fe–4S] unit by subtracting the contribution of the uncoupled [4Fe–4S] cluster from the raw data using these simulated spectra. Some of the prepared spectra are shown in Figure 5. (Contribution from the rhombic Fe(III) species has not been removed.) To further characterize the siroheme–[4Fe–4S] unit, we analyzed these prepared spectra with the following $S = {}^5/_2$ spin Hamiltonian:

$$\hat{H} = D\left[S_z^2 - S(S+1)/3 + \frac{E}{D}(S_x^2 - S_y^2)\right] + \beta\vec{S}\cdot\tilde{g}\cdot\vec{H} + \vec{S}\cdot\tilde{A}\cdot\vec{I} + \frac{eQV_{zz}}{12}[3I_z^2 - I(I+1) + \eta(I_x^2 - I_y^2)] - g_n\beta_n\vec{H}\cdot\vec{I} \quad (1)$$

For our analysis, we assumed that the coupled [4Fe–4S] cluster consisted of two pairs of equivalent iron sites and that the magnetic hyperfine coupling tensors, $\tilde{A}$, for the iron sites are isotropic. The assumption of two pairwise equivalent sites is supported by previous studies on iron–sulfur clusters,[27,28] and an isotropic A was reported for the cluster in *E. coli* sulfite reductase.[19] With these assumptions, analysis of the data was possible and the hyperfine parameters were determined with certainty. The value for E/D was obtained by the EPR measurements, the zero-field splitting D was determined from the strong-field Mössbauer spectra, the magnetic hyperfine coupling constants, A, were estimated from the total splitting of the weak-field spectra, the quadrupole splitting of the siroheme was inferred from the high-temperature data (see below), and the quadrupole splittings for the two pairwise iron sites were taken from the averaged values of the results of the least-squares fit for the uncoupled [4Fe–4S] cluster. The rest of the parameters were determined through a series of theoretical simulations and by visually comparing the simulations with experiments. The set of hyperfine parameters which yields theoretical spectra (solid lines in Figure 5) that best resemble the experimental data are listed in Table II. A particularly interesting result of this analysis is that the magnetic hyperfine coupling constants obtained for the coupled [4Fe–4S] cluster are strikingly similar to those found for the siroheme–[4Fe–4S] unit in *E. coli* sulfite reductase.[19] In order to explain the magnetic coupling constants observed in an intrinsically diamagnetic [4Fe–4S] cluster, Christner et al.[19] proposed a spin-coupling model in which the heme iron was coupled to each individual cluster iron. According to the model, the hyperfine coupling constants for the

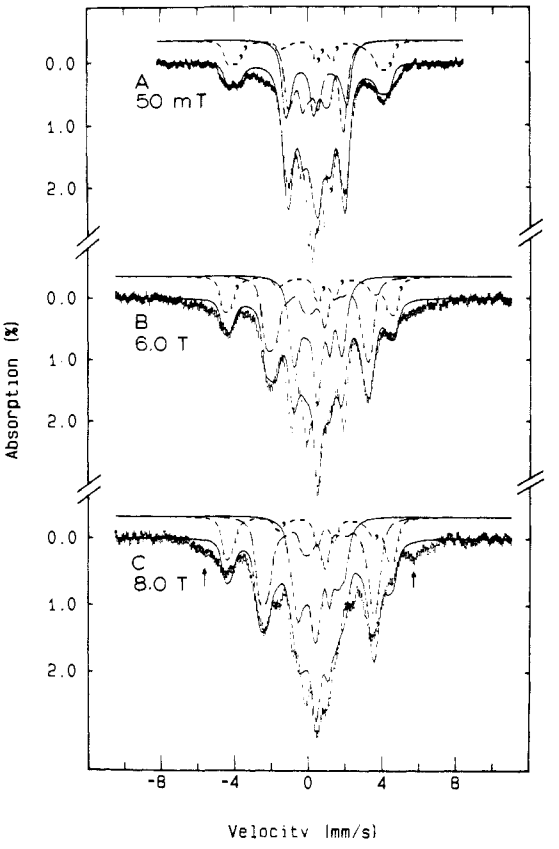

Figure 5. Mössbauer spectra of the exchange-coupled siroheme–[4Fe–4S] unit in desulforubidin from *D. baculatus* recorded at 4.2 K in parallel applied fields of the indicated strengths. These spectra were prepared by subtracting the 42% contribution of the diamagnetic $[4Fe-4S]^{2+}$ cluster from the raw data (see text). The contribution from the Fe(III) species has not been removed and is indicated by the arrows in C. The solid lines plotted over the data are theoretical simulations using the parameters listed in Table II. Theoretical spectra of the individual iron sites are also shown: siroheme, (---); site 1 of the [4Fe–4S] cluster, (– – –); site 2 of the [4Fe–4S] cluster, (—).

Table II. Spin-Hamiltonian Parameters for the Exchange-Coupled Siroheme–[4Fe–4S] Unit in the Native Desulforubidin from *D. baculatus*[a]

		[4Fe–4S]	
	siroheme	site 1	site 2
D, cm^{-1}	13.5 ± 1.5	13.5 ± 1.5	13.5 ± 1.5
E/D	0.02 ± 0.01	0.02 ± 0.01	0.02 ± 0.01
$A_{xx}/g_n\beta_n$,[b] T	−15.8 ± 0.5	5.2 ± 0.5	−5.2 ± 0.7
$A_{yy}/g_n\beta_n$, T	−16.5 ± 0.5	5.2 ± 0.5	−5.2 ± 0.7
$A_{zz}/g_n\beta_n$, T	−16.2 ± 1.0	5.2 ± 0.5	−5.2 ± 0.7
ΔE_Q, mm/s	2.0 ± 0.2	−0.9 ± 0.2	1.2 ± 0.2
δ, mm/s	0.47 ± 0.05	0.45 ± 0.02	0.45 ± 0.02
η[c]	0 ± 0.2	−2.0 ± 0.5	−3 ± 1

[a] The uncertainties were estimated by visually comparing the theoretical simulations with the experimental data. [b] The symbol β_n represents the nuclear magneton, and g_n has the values 0.1806 and −0.1033 for the ground and excited states of the ^{57}Fe nucleus. [c] $\eta = (V_{xx} - V_{yy})/V_{zz}$, where V_{ii} are the principal components of the electric field gradient tensor.

cluster irons depend on the exchange-coupling constants between the heme iron and the cluster irons. The fact that the A's for the clusters in desulforubidin and in *E. coli* sulfite reductase are almost identical suggests strongly that the exchange-coupling mechanism of the siroheme–[4Fe–4S] units in both reductases must be very similar. The differences observed in EPR measurements may reflect only variations in the immediate heme iron environment. These variations are further substantiated by the observation that the hyperfine coupling constant (16 T) obtained for the siroheme in desulforubidin is significantly smaller than the constant 20 T reported for *E. coli* sulfite reductase.[19] In fact, the magnitude

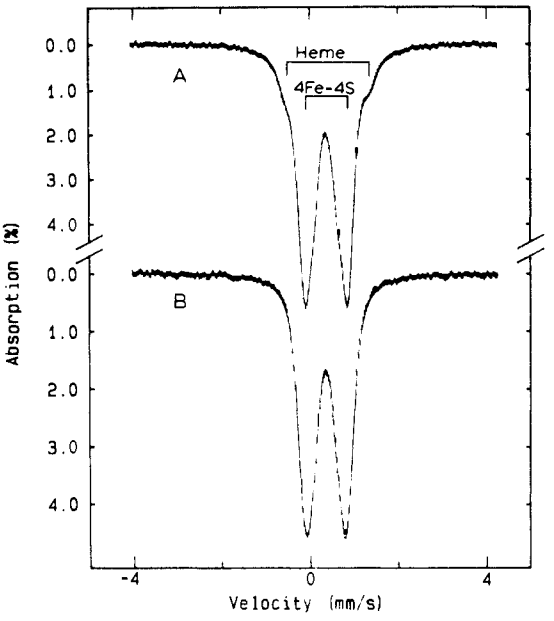

Figure 6. 195 K Mössbauer spectra of the as-isolated desulforubidin from *D. baculatus* (A) and desulfoviridin from *D. gigas* (B). The solid lines are least-squares fits of the data. Absorptions originating from the siroheme and the [4Fe–4S] cluster are indicated.

16 T is the smallest value ever reported for a high-spin ferric heme.

High-Temperature Mössbauer Studies of Native Proteins. At high temperatures (above 80 K), the electronic relaxation for iron protein is generally fast in comparison with the ^{57}Fe nuclear precession time. The Mössbauer spectra recorded at these temperatures consist of only quadrupole doublets. Consequently, the high-temperature Mössbauer spectrum is very useful for quantitative analysis in the case that the doublets are resolved. Figure 6 shows the 195 K spectra of desulforubidin (6A) and desulfoviridin (6B). Unfortunately, a broad and unresolved doublet is observed. However, in addition to the intense central doublet, desulforubidin exhibits shoulders at −0.5 and +1.4 mm/s. From the low-temperature studies reported above and from the measurements of the reduced enzymes presented below, we realized that the difference between these two reductases is the lack of siroheme in desulfoviridin. The extra shoulders observed for desulforubidin must be therefore originating from the siroheme. The central doublet is attributed to the [4Fe–4S] clusters, and the absorptions arising from the rhombic Fe(III) species are unresolved. For a detailed analysis, the desulfoviridin spectrum (6B) was fitted with four quadrupole doublets of equal intensity. The desulforubidin spectrum (6A) was fitted with five quadrupole doublets. The heme iron was assumed to have a different intensity from those of the cluster irons. For this analysis, the contribution of the Fe(III) species was neglected. The solid lines in Figure 6 represent the least-squares fit spectra and the calculated parameters are listed in Table I. The percent absorption for the siroheme in desulforubidin was found to be 8 ± 2%, which is in agreement with the results obtained from the reduced enzyme (see below). The absorptions for the siroheme in desulfoviridin and for the Fe(III) species were not determined in this analysis.

The EPR measurements indicate that the siroheme is high-spin ferric. The isomer shift obtained from the least-squares fit agrees with this assignment. The quadrupole splitting (1.94 mm/s) appears to be unusually large for high-spin ferric hemes and is twice as large as the value 1 mm/s found for the siroheme in *E. coli* sulfite reductase.[19] This observation again indicates dissimilarities between the hemes in the dissimilatory and the assimilatory sulfite reductases. Although high-spin ferric compounds generally yield small ΔE_Q, quadrupole splittings larger than 1.5 mm/s have been reported for quite a few high-spin ferric hemoproteins.[29-31]

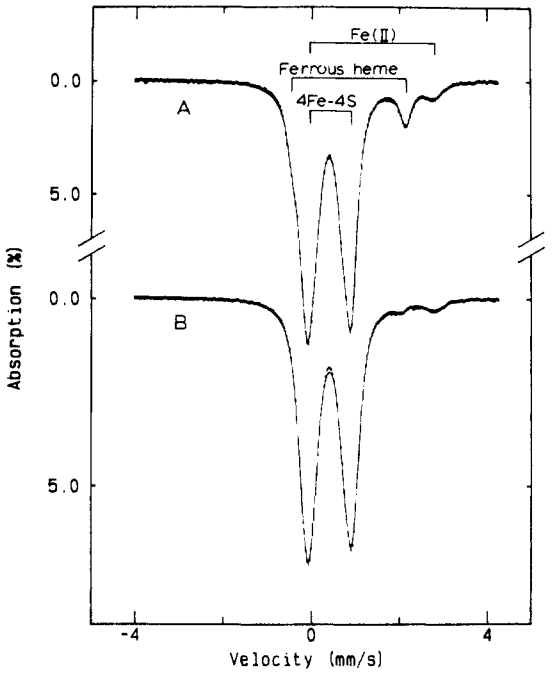

Figure 7. 150 K Mössbauer spectra of the reduced desulforubidin from *D. baculatus* (A) and desulfoviridin from *D. gigas* (B). The solid lines are least-squares fits of the data. Positions of the quadrupole doublets originating from different iron centers are indicated.

In our analysis of the low-temperature data, we assumed that the $[4Fe–4S]^{2+}$ cluster spectra for both reductases were identical. The Mössbauer parameters obtained at high temperatures indicate that within experimental uncertainties, the doublets originating from these clusters are practically the same and therefore support our assumption. The parameters listed in Table I also suggest that the [4Fe–4S] clusters in these two dissimilatory sulfite reductases are similar to the $[4Fe–4S]^{2+}$ clusters in *Chromatium* HiPIP[27] and *Bacillus stearothermophilus* ferredoxin.[28] In other words, the cluster spectrum can be decomposed into four quadrupole doublets with different splittings and is strongly temperature dependent. The spectrum for the iron–sulfur cluster in an exchange-coupled siroheme–[4Fe–4S] unit has also been reported for *E. coli* sulfite reductase[19] and for an assimilatory-type sulfite reductase from *D. vulgaris*.[9] In both cases, the cluster exhibits a sharp, temperature-independent quadrupole doublet, suggesting that all four iron sites in the cluster are equivalent. In order to examine whether or not the coupled [4Fe–4S] cluster in desulforubidin is similar to those in *E. coli* and *D. vulgaris* sulfite reductase, we attempted to fit the central doublet of the desulforubidin spectrum with five doublets. One of the doublets was assumed to have intensity equal to the sum of the other four. No satisfactory fit could be obtained with such an assumption. Consequently, the evidence suggests that the coupled [4Fe–4S] cluster in desulforubidin is similar to the uncoupled cluster and is ferredoxin-like.

Mössbauer Studies of Reduced Reductases. Under a hydrogen atmosphere and in the presence of trace quantities of hydrogenase and methylviologen, desulforubidin and desulfoviridin can be reduced and become EPR silent. In the absence of an external applied field, the Mössbauer spectra consist of only quadrupole doublets. In the presence of a strong applied field, large internal fields are induced at the iron sites of the reduced siroheme–[4Fe–4S] unit. These observations indicate that the reduced siroheme–[4Fe–4S] unit is an integer spin system with $S > 0$. (Detailed analysis of the strong-field spectra and identification of the spin state for the reduced siroheme–[4Fe–4S] unit will be the subjects of future reports.) Figure 7 shows the 150 K spectra

(29) Münck, E.; Champion, P. M. *J. Phys. (Les Ulis, Fr.)* **1974**, *35* (C6), 33–46.

(30) Emptage, M. H.; Zimmermann, R.; Que, L., Jr.; Münck, E.; Hamilton, W. D.; Orme-Johnson, W. H. *Biochim. Biophys. Acta* **1977**, *495*, 12–23.

(31) Lang, G. *Q. Rev. Biophys.* **1970**, *3*, 1–60.

Table III. Mössbauer Parameters for the Reduced Desulforubidin from *D. baculatus* and the Reduced Desulfoviridin from *D. gigas*

	reduced desulforubidin		reduced desulfoviridin	
siroheme	ΔE_Q, mm/s	δ, mm/s	ΔE_Q, mm/s	δ, mm/s
		T = 195 K		
siroheme [4Fe–4S]	2.47 ± 0.05	0.83 ± 0.03	2.3 ± 0.1	0.80 ± 0.06
site 1	1.11 ± 0.04	0.36 ± 0.03	1.17 ± 0.04	0.38 ± 0.03
site 2	0.93 ± 0.04	0.36 ± 0.03	0.96 ± 0.04	0.37 ± 0.03
site 3	0.87 ± 0.04	0.38 ± 0.03	0.88 ± 0.04	0.40 ± 0.03
site 4	0.54 ± 0.04	0.37 ± 0.03	0.58 ± 0.04	0.37 ± 0.03
Fe(II)	2.76 ± 0.07	1.20 ± 0.04	2.69 ± 0.07	1.19 ± 0.04
		T = 150 K		
siroheme [4Fe–4S]	2.56 ± 0.05	0.84 ± 0.03	2.4 ± 0.1	0.84 ± 0.06
site 1	1.15 ± 0.04	0.37 ± 0.03	1.20 ± 0.04	0.35 ± 0.03
site 2	0.96 ± 0.04	0.39 ± 0.03	0.97 ± 0.04	0.40 ± 0.03
site 3	0.94 ± 0.04	0.40 ± 0.03	0.93 ± 0.04	0.42 ± 0.03
site 4	0.60 ± 0.04	0.40 ± 0.03	0.64 ± 0.04	0.40 ± 0.03
Fe(II)	2.90 ± 0.07	1.20 ± 0.04	2.93 ± 0.07	1.21 ± 0.04
		T = 4.2 K		
siroheme [4Fe–4S]	2.72 ± 0.05	0.92 ± 0.03	2.7 ± 0.1	0.99 ± 0.06
site 1	1.38 ± 0.04	0.45 ± 0.03	1.44 ± 0.04	0.45 ± 0.03
site 2	1.10 ± 0.04	0.45 ± 0.03	1.16 ± 0.04	0.43 ± 0.03
site 3	1.02 ± 0.04	0.45 ± 0.03	1.04 ± 0.04	0.45 ± 0.03
site 4	0.71 ± 0.04	0.44 ± 0.03	0.73 ± 0.04	0.43 ± 0.03
Fe(II)	3.22 ± 0.07	1.25 ± 0.04	3.25 ± 0.07	1.24 ± 0.04

of reduced desulforubidin and desulfoviridin. Three distinct quadrupole doublets are observed and the high-energy lines of the doublets are resolved. A major difference between these two spectra is that the absorption peak at +2.1 mm/s is more intense for desulforubidin than for desulfoviridin. From the following analysis, we realized that this peak belongs to a doublet whose parameters are consistent with high-spin ferrous heme ($S = 2$) and is therefore attributed to the siroheme. The central doublet originates from the [4Fe–4S] clusters. The rightmost line is assigned to a high-spin Fe(II) species which should be the reduced state of the high-spin Fe(III) species found in the native enzymes. Each spectrum was fitted with six quadrupole doublets. Four of the doublets belonging to the [4Fe–4S] clusters were assumed to have equal intensity. The solid lines in Figure 6 are results of the least-squares fits. The parameters obtained are listed in Table III, including results obtained for different temperatures.

A most interesting and important result of the above analysis is the discovery of different siroheme contents in these two reductases. Since the siroheme spectrum is well resolved from the rest of the spectrum, its percent absorption can be determined with certainty. The percent absorption of the siroheme was found to be 10 ± 2% for desulforubidin and only 2 ± 1% for desulfoviridin. This result indicates unambiguously that desulforubidin contains approximately 5 times more siroheme in comparison with desulfoviridin, a result that is supported by the EPR studies and is consistent with the Mössbauer measurements of the native proteins. Correlating with the result of iron-content determination (21 irons per molecule of desulforubidin), 10% siroheme absorption yields ~2 sirohemes per molecule. This value is in good agreement with the chromophore content obtained by chemical determination. On the other hand, the 2% siroheme absorption for desulfoviridin yields only an average of 0.4 siroheme per molecule. Since about 2 sirohydrochlorins were extracted from each molecule, we concluded that 80% of the tetrahydroporphyrin chromophores in the purified desulfoviridin do not contain iron! Implications of this conclusion will be discussed in the following section.

The Mössbauer parameters obtained for the [4Fe–4S] clusters are almost indistinguishable from those of the clusters in the native enzymes, suggesting that the oxidation state of the cluster in the reduced enzymes remains at 2+. The siroheme parameters indicate that the heme is reduced into a high-spin ferrous state ($S = 2$). Consequently, under the above-mentioned reducing conditions, the siroheme–[4Fe–4S] unit in both dissimilatory sulfite reductases is reduced by one electron, and the electron is localized on the heme. Mössbauer measurements of the one-electron-reduced state of *E. coli* sulfite reductase have been reported.[32] It was also found that the state of the [4Fe–4S] cluster was unaltered when compared with the native enzyme, and the electron was also localized on the siroheme. However, in *E. coli* sulfite reductase the reduced siroheme was in an intermediate spin state ($S = 1$). Its spectrum is distinctively different from that of the reduced siroheme in desulforubidin or desulfoviridin. From the studies of the native enzymes, the siroheme environments of the two dissimilatory sulfite reductases were found to be different from that of the assimilatory sulfite reductase. The above results indicate further that the heme environments remain distinct in the one-electron-reduced enzymes.

Table IV. Wavelengths (nm) and Relative Intensities of the Absorption Maxima for *D. gigas* Desulfoviridin, *E. coli* Sulfite Reductase, and Metal-Free Tetrahydroporphyrin Methyl Ester[a]

D. gigas desulfovifidin	*E. coli* sulfite reductase	metal-free chromophore
380 (0.86)	386 (1.00)	375 (0.89)
390 (0.91)		385 (0.89)
408 (1.00)	455 (0.57)	403 (1.00)
583 (0.21)	587 (0.23)	570 (0.15)
628 (0.42)	714 (0.07)	617 (0.28)

[a] The data are taken from ref 12. Relative intensities are enclosed in parentheses.

The Mössbauer parameters of the high-spin Fe(II) species are consistent with adventitiously bound impurity irons found in protein samples. In fact, the 4.2 K values ($\Delta E_Q = 3.2$ mm/s and $\delta = 1.25$ mm/s) are identical with those reported for Fe(II) in buffer solution.[33] However, these values are common for octahedrally coordinated Fe(II) compounds[34] and are not unique for adventitious iron. Presently, we are perplexed by the facts that this species exists in both dissimilatory sulfite reductases and quantitates to approximately one iron per molecule.

Discussion

In the previous section, we have presented some chemical, optical, EPR, and Mössbauer data of two dissimilatory sulfite reductases isolated from sulfate-reducing bacteria, namely, desulforubidin from *D. baculatus* and desulfoviridin from *D. gigas*. The data indicate that both reductases contain equal amounts of [4Fe–4S] clusters (four clusters per molecule) but have different contents of siroheme. Desulforubidin contains two sirohemes per molecule, and each siroheme is exchange-coupled to an [4Fe–4S] cluster (i.e., two of the four clusters are uncoupled). For desulfoviridin an average of 0.4 siroheme per molecule was found. Taking into consideration all the experimental evidence, we reach the conclusion that 80% of the tetrapyrrolic chromophores in desulfoviridin do not contain iron. Our data suggest that the purified desulfoviridin is inhomogeneous with respect to the distribution of the prosthetic groups. Depending on the distribution of the sirohemes, 60–80% of the desulfoviridin molecules contain only metal-free tetrahydroporphyrins while 20–40% of the enzyme molecules contain two to one sirohemes per molecule. In the earlier studies,[12,13] investigators were puzzled by the observation that metal-free tetrahydroporphyrins were extracted from desulfoviridin while sirohemes were extracted from *E. coli* sulfite reductase, from desulforubidins, and from P-582. The present finding not only can explain this puzzling observation but is also consistent with the distinct optical spectrum observed for desulfoviridin. In Table IV we compare the relative intensities and wavelengths of the absorption maxima of *D. gigas* desulfoviridin with those of the *E. coli* sulfite reductase and of the demetalized siroheme esters in methanol–H_2SO_4.[12] It is obvious from this comparison that

(32) Christner, J. A.; Münck, E.; Janick, P. A.; Siegel, L. M. *J. Biol. Chem.* **1983**, *258*, 11147–11156.
(33) Kent, T. A.; Dreyer, J. L.; Kennedy, M. C.; Huynh, B. H.; Emptage, M. H.; Beinert, H.; Münck, E. *Proc. Natl. Acad. Sci. U.S.A.* **1982**, *79*, 1096–1100.
(34) Menil, F. *J. Phys. Chem. Solids* **1985**, *46*, 763-789.

the optical spectrum of desulfoviridin resembles the metal-free tetrahydroporphyrin methyl ester and is distinct from the *E. coli* sulfite reductase.

The exchange-coupled siroheme–[4Fe–4S] unit was first reported in *E. coli* sulfite reductase,[19] and extensive spectroscopic studies have been performed to characterize this unit.[32,35-39] The coupling between the siroheme and the cluster was found to be retained in all the oxidation and ligation states examined. A recent X-ray crystallographic study indicates that the two prosthetic groups are bridged by a common ligand, probably a cysteine S_γ.[40] This work shows that the siroheme–[4Fe–4S] unit in desulforubidin exhibits properties that are both similar and dissimilar to those of the coupled unit in *E. coli* sulfite reductase. In the native enzymes, both units are composed of a high-spin ferric $S = {}^5/_2$ siroheme exchange-coupled to an intrinsically diamagnetic $S = 0$ $[4Fe–4S]^{2+}$ cluster. The magnetic hyperfine coupling constants, A, of the cluster irons obtained for both enzymes are almost identical. Since the A's of the cluster irons are induced from the paramagnetic siroheme through the exchange interaction, the observation of identical hyperfine constants indicates a similar exchange-coupling mechanism. The bridging ligand and the geometrical arrangement between the siroheme and the cluster may be the same in both units; however, the local environments surrounding the iron sites were found to be different. These variations are reflected in the differences observed in the EPR spectra, in the quadrupole splittings and the A values of the sirohemes, and in the ΔE_Q's of the cluster irons.

Under reducing conditions, the siroheme–[4Fe–4S] unit in desulforubidin can be reduced by one electron. The electron is localized in the siroheme and the ferric siroheme is reduced to a ferrous state. The [4Fe–4S] cluster remains in the 2+ state. Similar behavior was also reported for the one-electron-reduced *E. coli* sulfite reductase;[35] however, the electronic spin states of the ferrous sirohemes are different: $S = 2$ for desulforubidin and $S = 1$ for *E. coli* sulfite reductase. In *E. coli* sulfite reductase, the midpoint oxidation–reduction potentials for the siroheme and the cluster differ only by 65 mV.[39] Consequently, coexistence of one-electron- and two-electron-reduced states is obtained under reducing conditions. Fully reduced (two-electron-reduced) enzymes can be prepared under an Ar atmosphere in the presence of deazaflavin, EDTA, and light.[36] In the case of desulforubidin, we were not successful in producing the corresponding two-electron-reduced state. The reduced desulforubidin reported in this work is in a pure one-electron-reduced state. For this to occur the redox potentials of the siroheme and the coupled cluster in desulforubidin must differ by at least 100 mV. Since the one-electron-reduced state is the active state of the enzyme, detailed Mössbauer studies of the reduced desulforubidin should yield information of physiological significance and are the subjects of a future publication. We are also exploring different reduction methods in order to attain the two-electron-reduced state, and we are attempting to determine the redox potentials of the siroheme and the clusters using a redox-titration technique.

After the discovery of the exchange-coupled siroheme–[4Fe–4S] unit in *E. coli* sulfite reductase,[19] spectroscopic evidence for the existence of a siroheme–[4Fe–4S] unit was reported for spinach sulfite reductase[41] and for spinach nitrite reductase,[42] which possesses sulfite reductase activity.[43] More recently, an assimilatory-type sulfite reductase isolated from *D. vulgaris* was also found to contain a coupled siroheme–[4Fe–4S] unit.[9] The present studies further indicate that desulforubidin, a dissimilatory sulfite reductase, also contains a similar siroheme–[4Fe–4S] unit. These observations strongly suggest that the siroheme–[4Fe–4S] unit is a common prosthetic group and is the active site for sulfite and nitrite reduction. Interestingly, we found evidence that a majority of the purified desulfoviridin contains metal-free tetrahydroporphyrin and that only a minor portion of the purified enzymes contains the siroheme–[4Fe–4S] unit. Consequently, an important question to ask is could the existence of sirohydrochlorin be a result of damage caused by protein purification and be an artifact? Perhaps the observed enzymatic activity results from those proteins containing the coupled siroheme–[4Fe–4S] unit. Due to the following consideration we believe that this is not the case. Small molecules, such as CN^- or CO, form complexes with desulforubidin and with *E. coli* sulfite reductase. They were shown to coordinate to the siroheme group and inhibit the sulfite reduction activity;[37,39] however, these ligands do not inhibit the sulfite reduction activity of desulfoviridin.[44] As the siroheme–[4Fe–4S] cluster unit in desulfoviridin is similar to that in desulforubidin or in *E. coli* sulfite reductase, it is expected to complex with CO or CN^-. The fact that neither CO nor CN^- inhibits desulfoviridin suggested that the enzymatic activity originates from the enzyme molecules containing sirohydrochlorins. We have also performed preliminary Mössbauer studies on other dissimilatory sulfite reductases, namely, desulforubidin from *D. baculatus* strain Norway 4 and desulfoviridin from *D. desulfuricans* strain ATCC 27774. These preliminary investigations indicate that metal-free tetrahydroporphyrins are commonly present in desulfoviridin. Furthermore, if the sirohemes were solely responsible for activity, one would expect desulfoviridin to exhibit about 20% of the activity found with desulforubidin. In fact, *D. gigas* desulfoviridin was reported to be more active than *D. baculatus* desulforubidin.[3] A survey of the specific activities of both types of reductases shows that there is no correlation with the nature of the prosthetic group. Finally, the 628-nm absorption peak, as we have noted, appears to be related to the presence of sirohydrochlorin in desulfoviridin. It is seen in bacterial crude extracts and its intensity does not increase in the course of protein purification. Observation of the 628-nm peak has also been reported for whole bacterial cells.[45]

Acknowledgment. We thank Mr. Jeffrey Levy for writing the program to plot the Mössbauer figures, and we also thank the National Institutes of Health for a research career development award (Grant AM01135) to B.H.H. and a grant from the NSF/CNRS fellowship program to G.F. This work was supported by the National Science Foundation (Grants PCM-8305995 and DMB-8614290 to B.H.H., DMB-8602789 to J.L.G., and PCM-8213874 to D.V.D.), by the U.S. Department of Energy (Grant DE-A509-80ER 10499 to H.D.P.), and by the Instituto National de Investigação Cientifica, Junta Nacional de Investigação, Cientifica e Tecnologica and Agency for International Development (I.M.).

Registry No. Fe, 7439-89-6; desulforubidin, 42612-25-9; desulfoviridin, 9045-15-2; bisulfite reductase, 9059-42-1; siroheme, 52553-42-1; sirohydrochlorin, 65207-12-7.

(35) Christner, J. A.; Janick, P. A.; Siegel, L. M.; Münck, E. *J. Biol. Chem.* **1983**, *258*, 11157–11164.
(36) Janick, P. A.; Siegel, L. M. *Biochemistry* **1982**, *21*, 3538–3547.
(37) Janick, P. A.; Siegel, L. M. *Biochemistry* **1983**, *22*, 504–515.
(38) Christner, J. A.; Münck, E.; Kent, T. A.; Janick, P. A.; Salerno, J. C.; Siegel, L. M. *J. Am. Chem. Soc.* **1984**, *106*, 6786–6794.
(39) Siegel, L. M.; Rueger, D. C.; Barber, M. J.; Krueger, R. J.; Orme-Johnson, N. R.; Orme-Johnson, W. H. *J. Biol. Chem.* **1982**, *257*, 6343–6350.
(40) McRee, D. E.; Richardson, D. C.; Richardson, J. S.; Siegel, L. M. *J. Biol. Chem.* **1986**, *261*, 10277–10281.
(41) Krueger, R. J.; Siegel, L. M. *Biochemistry* **1982**, *21*, 2905–2909.
(42) Wilkerson, J. O.; Janick, P. A.; Siegel, L. M. *Biochemistry* **1983**, *22*, 5048–5054.
(43) Krueger, R. J.; Siegel, L. M. *Biochemistry* **1982**, *21*, 2892–2904.
(44) Ishimoto, M.; Yagi, T. *J. Biochem. (Tokyo)* **1961**, *49*, 103–109.
(45) Postgate, J. R. *J. Gen. Microbiol.* **1956**, *14*, 545–572.